Wetting on a Spherical-Shell Substrate

Ioannis A. Hadjiagapiou†

Solid State Physics Section, Department of Physics, University of Athens, Panepistimiopolis, Zografos GR 157-84, Athens, Greece

Received: November 15, 1996; In Final Form: March 10, 1997⊗

A density-functional theory for the wetting of an inert spherical-shell substrate by a single-component bulk vapor is developed, on the basis of the usual assumption that the pairwise intermolecular interaction is divided into a repulsive hard sphere and a weak attractive part. The substrate vapor−molecule pairwise interaction is also divided into a hard-wall repulsive interaction and a weak attractive tail. Choosing the attractive interactions properly, a second-order nonlinear functional differential equation results, which is solved numerically with appropriate boundary conditions. It is shown that the wetting layer, formed on the adsorbent, is either a thin or a thick film of finite thickness. Furthermore, in some cases the substrate is not at all wet. The wall−vapor and other interfacial tensions, the associated radii, and the principal tensors (the transverse $p_T(r)$ and normal $p_N(r)$) are also calculated. The wall−vapor interface is mainly under tension ($p_N(r) > p_T(r)$).

1. Introduction

The behavior of fluids adsorbed on solid substrates is of fundamental and practical interest in such diverse fields as tertiary oil recovery, phase and film growth, lubricants, textile fibers, dyeing, crystallization, etc.

The solid substrate (simply, wall) is considered to consist of a large number of spherical molecules on lattice sites whose interactions are added to form the external field, $V_{ext}(\mathbf{r})$, not affected by the bulk fluid phase. The wall molecules are assumed to form a continuum of uniform number density n_S, thus $V_{ext}(\mathbf{r})$ is calculated by integrating over substrate, i.e.,

$$V_{ext}(\mathbf{r}) = n_s \int_\Sigma \Phi_{SF}(|\mathbf{r}-\mathbf{r}'|)\, d\sigma' \tag{1.1}$$

where $\Phi_{SF}(|\mathbf{r}-\mathbf{r}'|)$ is the pairwise potential between a fluid-molecule at $\mathbf{r}$ and a wall-molecule at $\mathbf{r}'$, $d\sigma'$ the integration measure, and Σ the domain of integration (volume, surface, line). $V_{ext}(\mathbf{r})$ will be identified with the attractive part of the wall−fluid interactions, because the interfacial properties that will be examined are not affected by the short-range wall−fluid repulsive interactions.[1]

Most theoretical studies on wetting of solid substrates concern the growth of wetting layers on planar walls; such a geometry is convenient for calculations, while less attention has been devoted to curved substrates. In the present case we are concerned with the wetting of a spherical-shell substrate (of radius R) by a bulk fluid phase within the mean field theory (MFT). The wall−fluid forces play an important role in controlling the wetting behavior on the wall, and the adsorbed phase can be either vapor or liquidlike depending on the wall−fluid forces. The wall molecules are distributed uniformly only on the wall surface; thus the integral in (1.1) is now a surface one, i.e.

$$V_{ext}(\mathbf{r}) = n_s \int_S \Phi_{SF}(|\mathbf{r}-\mathbf{r}'|)\, dS \tag{1.2}$$

$$= n_s R^2 \int_S \Phi_{SF}(|\mathbf{r}-\mathbf{r}'|) \sin\vartheta'\, d\vartheta'\, d\varphi'$$

where ϑ' and φ' are the angular variables and $\Phi_{SF}(|\mathbf{r}-\mathbf{r}'|)$ is considered to be spherically symmetric. The spherical substrate is embedded in a solvent that is in the vapor phase, bulk fluid; thus, in the theoretical treatment, the fluid molecules and the wall can be considered as forming a limiting binary mixture in the sense that the concentration of one of its components (solute component) vanishes. When the radius R of the spherical wall is infinitely large in comparison with the radius d of the fluid molecules, the system becomes equivalent to a planar wall with a bulk fluid.[1]

When the substrate is planar and the bulk phase is vapor, then, at coexistence conditions, the adsorbent can be completely wet by a liquidlike film of infinite thickness (wetting class I), partially wet by a finite-thickness film (wetting class II), or nonwet[1] (wetting class III). Such a system can undergo a transition from one wetting class to another by varying a parameter,[1−3] e.g., temperature T. However, when the substrate is spherical, the wetting layer cannot be infinitely thick, so any phase transition is between a thin and a thick film and vice versa, i.e., the curvature restricts the wetting layer to finite thickness. This behavior must be allowed for in Antonov rule for the wall−vapor (γ_{WV}), wall−liquid (γ_{WL}), and liquid−vapor (γ_{LV}), surface tensions (for complete wetting in the planar limit[4])

$$A_R\gamma_{WV} = A_R\gamma_{WL} + A_{R+l}\gamma_{LV} \tag{1.3}$$

where A_R and A_{R+l} are the surface areas of the spheres with radii R and $(R + l)$, respectively; $(R + l)$ is the distance where the density $\rho(r)$ attains its bulk value ρ_v and l is the thickness of the wetting layer. In case of a large adsorbing wall, (1.3) yields

$$\gamma_{WV} = \gamma_{WL} + (A_{R+l}/A_R)\gamma_{LV}$$

$$\cong \gamma_{WL} + \left(1 + \frac{2l}{R}\right)\gamma_{LV} \tag{1.4a}$$

recovering the planar limit result as $R \to \infty$ for complete wetting, i.e.

$$\gamma_{WV} = \gamma_{WL} + \gamma_{LV} \tag{1.4b}$$

† E-mail: ihatziag@atlas.uoa.gr.

⊗ Abstract published in *Advance ACS Abstracts,* August 15, 1997.

S1089-5647(96)03816-3 CCC: $14.00

Holyst and Poniewierski[4] found that for finite R the wetting transition is neither of first or second order; the film thickness l varies as ln R for large R and $T_W > T_W^\infty$ (T_W and T_W^∞ the wetting temperature in spherical and planar geometry, respectively). Applying Landau-type theory for cylindrical and spherical geometries, Gelfand and Lipowski[5] found that complete and critical wetting are suppressed in cylindrical and spherical substrates. Upton et al.[6] calculated the phase diagrams, at coexistence, for wetting on the above curved substrates; they also found that l behaves as $\xi \ln(R/\xi)$ for $R \gg \xi$ and as ξ for $R \ll \xi$ (ξ bulk correlation length of the adsorbate).

The density-functional approach, used in this study, is based on Sullivan's model for the fluid−fluid and wall−fluid pairwise interaction potentials; this model was applied initially to the study of adsorption on a planar wall from a single- and two-component fluid.[1−3] This model is now applied to the case of a spherical substrate when the bulk phase is vapor at reduced temperature $T^* = T/T_c = 0.8$, where T_c is the bulk critical temperature. The advantage of this theory is that it yields results well suited for numerical calculations.

The purpose of the current work is to explore the wetting behavior of a spherical substrate by a bulk gas; although this calculation is based on a simple model, it nevertheless gives results that can elucidate some basic properties of a real system, as in the planar geometry[1−3] or spherical drops.[7] The paper is arranged as follows: in section 2 the system is defined through a density-functional grand potential, which, after minimization, gives the differential equation for the density profile; the expressions for the pressure tensor and the surface tensions with the associated radii are also found. The numerical calculations and discussions follow in section 3 and the conclusions in section 4.

2. Theory

2.1. Density Profile. The grand potential functional for a single-component fluid in an external field $V_{ext}(\mathbf{r})$ at temperature T can be written as

$$\Omega_V[\rho(\mathbf{r})] = \int_V \left\{ f_h[\rho(\mathbf{r})] + \left(\frac{1}{2}\right)\rho(\mathbf{r}) \int_V \rho(\mathbf{r})\, w(|\mathbf{r}-\mathbf{r}'|)\, d\mathbf{r}' + (V_{ext}(\mathbf{r}) - \mu)\rho(\mathbf{r}) \right\} d\mathbf{r} \quad (2.1)$$

where $\rho(\mathbf{r})$ is the average number density at $\mathbf{r}$ of the fluid molecules, μ the bulk vapor chemical potential, and V the volume of the system. The repulsive force contribution to the Helmholtz free energy is treated in the local density approximation in that $f_h[\rho(\mathbf{r})]$ is the Helmholtz free energy density of a uniform hard-sphere fluid at density $\rho(\mathbf{r})$, while the long-range attractive forces between fluid molecules are treated in the mean field approximation; i.e., $w(r)$ is the attractive part of the pairwise potential between two fluid molecules. From the variational principle $\delta\Omega_V[\rho(\mathbf{r})]/\delta\rho(\mathbf{r}) = 0$ the equilibrium density $\rho(\mathbf{r})$ is calculated as a solution of the corresponding Euler−Lagrange integral equation

$$\mu = V_{ext}(\mathbf{r}) + \mu_h[\rho(\mathbf{r})] + \int_V \rho(\mathbf{r}')\, w(|\mathbf{r}-\mathbf{r}'|)\, d\mathbf{r}' \quad (2.2)$$

where $\mu_h[\rho(\mathbf{r})] = \partial f_h[\rho(\mathbf{r})]/\partial\rho(\mathbf{r})$ is the hard-sphere chemical potential. Choosing properly the potentials $V_{ext}(\mathbf{r})$ and $w(r)$, the integral equation (2.2) can be converted to a functional nonlinear second-order differential equation with appropriate boundary conditions. Following Sullivan[1]

$$w(r) = -(\alpha\lambda^3/4\pi)e^{-\lambda r}/\lambda r \quad (2.3)$$

where λ is an inverse range length for fluid-fluid interaction, chosen such that $\lambda d = 1$, r is the distance between two fluid molecules, d is the diameter of the bulk-vapor particles and α is given by

$$\alpha = -\int_V w(r)\, d\mathbf{r} \quad (2.4)$$

which is a measure of the integrated strength of the attractive intermolecular interaction.

For the sake of simplicity, all the subsequent quantities and equations are transformed to dimensionless units

$$\mu^* = \beta\mu,\ p^* = \beta d^3 p,\ T^* = T/T_c,\ \gamma^* = \beta d^2\gamma,\ R^* = \lambda R,\ r^* = \lambda r,\ \alpha^* = \beta\alpha/d^3 = 11.102/T^*,\ \rho^* = \rho d^3,\ V^*(r) = \beta V(r),\ \Gamma^* = d^2\Gamma \quad (2.5a)$$

although the asterisks will be suppressed. γ is the surface tension, p the pressure, $\beta = (k_B T)^{-1}$, k_B Boltzmann's constant, and Γ the total adsorption (surface excess density) defined by

$$\Gamma = \int_R^\infty \frac{r^2}{R^2}(\rho(r) - \rho_V)dr \quad (2.5b)$$

If a wall molecule interacts with a fluid molecule via a Yukawa potential $\Phi_{SF}(r) = -Ce^{-\lambda_w r}/(\lambda_w r)$, where λ_W (wall−fluid inverse range parameter) and C are positive constants, then the integrated wall−fluid interaction due to the totality of the surface molecules of the substrate is obtained via (1.2) as

$$V_{ext}(r) = \infty \qquad r < R$$
$$= -\epsilon_w \frac{R}{r} e^{-r} \sinh R \qquad r \geq R \quad (2.6)$$

where $\lambda_W = \lambda$, assuming that the range of the intermolecular interactions is the same as that of the wall−fluid interactions. ϵ_W is proportional to n_S and C; it is a measure of the well depth for the wall−vapor interaction. In order to relate ϵ_W to the specific wall−vapor pair under consideration, it is usually expressed in terms of parameters referring to the separate vapor and substrate phases. Such a relation is given by[8]

$$\epsilon_W = (\epsilon_{FF}\epsilon_{WW})^{1/2}\left(\frac{\sigma_{FF}\sigma_{WW}}{\sigma_{FW}^2}\right)^3 \quad (2.7a)$$

constituting a combination of the geometric rule for the interaction energies (Berthelot rule) and arithemtic rule (Lorentz rule) for the hard-core diameters. The parameters ϵ_{FF} and ϵ_{WW} are the minima in the fluid−fluid and wall−wall interaction potentials, respectively; σ_{FF} and σ_{WW} are the associated hard-core diameters of the particles in the respective phases, and

$$\sigma_{FW} = (\sigma_{FF} + \sigma_{WW})/2 \quad (2.7b)$$

is the arithmetic mixing rule.[8] If the bulk phase remains the same, then varying ϵ_W implies either a new substrate or a variation in the nature (structural, chemical, etc.) of the substrate,[9] for ϵ_W is temperature independent.[1] It can assume any positive value and is characteristic of the substrate, as long as $\lambda_W = \lambda = d^{-1}$. A distinguishing feature of the potential (2.6) is that its strength (the part that is separated from the distance dependence, i.e., $\epsilon_W R \sinh R$) depends strongly on the substrate's radius R. Substituting the potentials (2.3) and (2.6) into (2.2) and differentiating twice with respect to r yields

$$\mu_h''[\rho(r)] + \frac{2}{r}\mu_h'[\rho(r)] - \mu_h[\rho(r)] + \mu = -\alpha\rho(r) \quad (2.8)$$

where the prime denotes the derivative with respect to r. This equation is a functional differential equation, since it depends on $\rho(r)$ and is identical to that found earlier in the study of spherical drops using Sullivan's model,[7] but now the second term in the left-hand side is well-behaved since r is always greater than zero, or similar to that for a planar substrate.[1,2]

The solution to (2.8) is uniquely defined if supplemented by the appropriate boundary conditions. In the limit $r \rightarrow \infty$

$$\mu_h(r) \rightarrow \mu_{h,v}, \quad \mu_h'(r) \rightarrow 0 \tag{2.9a}$$

where $\mu_{h,v} = \mu_h(\rho_v)$ is the bulk-phase hard-sphere chemical potential; the boundary condition on the substrate is

$$\mu_h'[\rho(R)] = (\mu_h[\rho(R)] - \mu)\left(\coth R - \frac{1}{R}\right) - \epsilon_W \tag{2.9b}$$

by differentiating (2.2) once with respect to r and evaluating it at $r = R$.

Adopting the Carnahan−Starling approximation for hard spheres, the hard-sphere pressure is given by

$$p_h(\rho) = \rho k_B T \frac{1 + \eta + \eta^2 - \eta^3}{(1 - \eta)^3} \tag{2.10a}$$

where $\eta = \pi\rho d^3/6$ is the packing fraction and the hard-sphere chemical potential is given by

$$\mu_h(\rho) = k_B T\left(\ln(\eta) + \frac{8\eta - 9\eta^2 + 3\eta^3}{(1 - \eta)^3}\right) \tag{2.10b}$$

Substituting (2.10b) into (2.8) yields

$$\eta''(r) = -\frac{2}{r}\eta'(r) - B_1(\eta)\eta'^2(r) - B_2(\eta) + B_3(\eta)\eta(r) \tag{2.11}$$

subject to the boundary conditions resulting from (2.9a,b)

$$\eta'(R) = \left\{(\mu_h[\eta(R)] - \mu)\left(\coth R - \frac{1}{R}\right) - \epsilon_W\right\}/A_1(\eta(R)) \tag{2.12a}$$

$$\eta(\infty) = \eta_V, \quad \eta'(\infty) = 0 \tag{2.12b}$$

where

$$A_1(\eta) = \frac{\partial(\beta\mu_h)}{\partial\eta} = \frac{1}{\eta} + \frac{8 - 2\eta}{(1 - \eta)^4},$$

$$A_2(\eta) = \frac{\partial A_1(\eta)}{\partial\eta} = -\frac{1}{\eta^2} + \frac{30 - 6\eta}{(1 - \eta)^5} \tag{2.13a}$$

$$B_1(\eta) = \frac{A_2(\eta)}{A_1(\eta)}, \quad B_2(\eta) = \frac{\beta\mu - \beta\mu_h(\eta)}{A_1(\eta)}, \quad B_3(\eta) = \frac{6\alpha\beta}{\pi A_1(\eta)} \tag{2.13b}$$

Initially, the coexisting bulk densities ρ_V and ρ_L are calculated for various T's by solving the simultaneous equations

$$p(\rho_V) = p(\rho_L), \quad \mu(\rho_V) = \mu(\rho_L) \tag{2.14}$$

for $T = 0.8$, resulting in $\rho_V = 0.041\,478$ and $\rho_L = 0.586\,731$.

2.2. Pressure Tensor and Surface Tension. In the nonuniform interfacial region, the pressure tensor $\boldsymbol{p}(\mathbf{r})$ is anisotropic and the mechanical equilibrium of the fluid under the external field $V_{ext}(r)$ is expressed by the equation

$$\nabla\cdot\boldsymbol{p}(\mathbf{r}) = -\rho(\mathrm{r})\nabla V_{ext}(r) \tag{2.15}$$

which does not define $\boldsymbol{p}(\mathbf{r})$ uniquely, although its divergence (2.15) is well-defined.[10] On symmetry grounds, $\boldsymbol{p}(\mathbf{r})$ depends only on r and is decomposed into

$$\boldsymbol{p}(\mathrm{r}) = p_N(r)[\hat{\mathbf{e}}_r\hat{\mathbf{e}}_r] + p_T(r)[\boldsymbol{I} - \hat{\mathbf{e}}_r\hat{\mathbf{e}}_r] \tag{2.16}$$

where $\boldsymbol{I}$ is the (3×3) unit tensor, $\hat{\mathbf{e}}_r$ the unit vector along $\mathbf{r}$ and $p_N(r)$, $p_T(r)$ the normal and tangential components of $\boldsymbol{p}(r)$, respectively, which also depend only on r; both vary significantly in the interfacial region and tend to p_V (bulk vapor pressure) as $r \rightarrow \infty$. Substituting (2.16) into (2.15) yields

$$p_N'(r) = \frac{2}{r}(p_T(r) - p_N(r)) - \rho(r)V_{ext}'(r) \tag{2.17}$$

where the prime denotes derivative with respect to r. Equation (2.17) can be integrated to yield the virial expression for the pressure difference Δp, i.e.

$$\Delta p = \int_R^\infty \left\{\frac{2}{u}[p_N(u) - p_T(u)] + \rho(\mathrm{u})V_{ext}'(u)\right\}\mathrm{d}u \tag{2.18}$$

In addition, once $p_T(r)$ is known, (2.17) yields the $p_N(r)$ component,

$$p_N(r) = \frac{R_T^2}{r^2}p_N(R_T) + \frac{1}{r^2}\int_{R_T}^r [2up_T(u) - u^2\rho(u)\,V_{ext}'(u)]\mathrm{d}u \tag{2.19}$$

where R_T is the radial distance from the origin of the axes where the density $\rho(r)$ attains its bulk value ρ_V and $p_N(R_T) = p_V$. The tangential component $p_T(r)$ can be identified with minus the grand potential free energy density[7]

$$p_T(r) = p_h(\rho_0(r)) + \left(\frac{1}{2}\right)\rho_0(r)[\mu - \mu_h(\rho_0(r)) - V_{ext}(r)] \tag{2.20}$$

where $\rho_0(r)$ is the equilibrium density.

By introducing the surface tension $\gamma(R_d)$ for an arbitrary dividing surface with radius R_d, (2.18) may be rewritten as

$$\Delta p = \frac{2\gamma(R_d)}{R_d} + \left(\frac{\partial\gamma(R_d)}{\partial R_d}\right)_{T,\mu} + \int_R^\infty \rho(u)\,V_{ext}'(\mathrm{u})\,\mathrm{du} \tag{2.21}$$

which is the generalized Laplace formula. Integrating again (2.17), it can also be found for an arbitrary dividing surface with radius R_d[10]

$$\Delta p = \frac{2\gamma(R_d)}{R_d} + \left(\frac{\partial\gamma(R_d)}{\partial R_d}\right)_{T,\mu} + \int_R^\infty \left(\frac{r}{R_d}\right)^2 \rho(r)\,V_{ext}'(r)\,\mathrm{d}r \tag{2.22}$$

which is another expression for the generalized Laplace equation. For the particular choice of the surface of tension, with radius $R_d = R_s$, (2.21 and 2.22) yield, respectively,

$$\Delta p = \frac{2\gamma_s}{R_s} + \int_R^\infty \rho(u)\,V_{ext}'(u)\,\mathrm{d}u \tag{2.23a}$$

$$\Delta p = \frac{2\gamma_s}{R_s} + \int_R^\infty \left(\frac{r}{R_s}\right)^2 \rho(r)\,V_{ext}'(r)\,\mathrm{d}r \tag{2.23b}$$

where $\gamma_s = \gamma(R_d = R_s)$. Although the last two relationships provide a definition of the surface of tension, separate definitions for γ_s and R_s are required as well; the mechanical route gives for γ_s[10]

$$\gamma_s = \int_R^\infty \left(\frac{u}{R_s}\right)^{-1} [p_N(u) - p_T(u)]\, du \tag{2.24}$$

Comparing (2.23a) and (2.23b), they yield

$$R_s^2 = \int_R^\infty r^2 \rho(r)\, V'_{ext}(r)\, dr \Big/ \int_R^\infty \rho(r)\, V'_{ext}(r)\, dr \tag{2.25}$$

In addition to the surface of tension, another dividing surface is used; this is the equimolar surface with radius R_e given by

$$R_e^3 = \frac{1}{\eta_V - \eta_L}\left[\int_R^\infty u^3 \frac{d\eta}{du}\, du + R^3(\eta(R) - \eta_L)\right] \tag{2.26}$$

The wall density $\eta(R)$ is, in general, significantly different from η_L, the packing fraction of the liquid phase at the same temperature and chemical potential as η_V; the respective surface tension ge is calculated from

$$\frac{\gamma_e}{\gamma_s} = \frac{2R_e}{3R_s} + \frac{1R_s^2}{3R_e^2} \tag{2.27}$$

For the spherical wall−fluid interface, the surface excess grand potential Ω_{ex} per unit area does not coincide with the surface tension, because of curvature and external field contributions, but splits into an external field term, a surface tension one, and a term proportional to the deviation of the normal component p_N at the wall from the bulk pressure, i.e.

$$\frac{\Omega_{ex}}{4\pi R^2} = \frac{1}{3}\gamma + \frac{R}{3}[p_N(R) - p] - \frac{1}{3R^2}\int_R^\infty u^3 \rho(u)\, V'_{ext}(u)\, du \tag{2.28a}$$

$$\gamma = \int_R^\infty \left(\frac{u}{R}\right)^2 [p_N(u) - p_T(u)]\, du \tag{2.28b}$$

where use has been made of (2.17). The latter relation is the wall−vapor surface tension γ_{WV} according to the virial route; it depends upon the choice of the pressure tensor, and consequently, the calculation of Ω_{ex} in (2.28a) is questionable. However, apart from the virial route to fluids, the compressibility route may also be applied fluids. This route, although more demanding, is free from the pressure tensor ambiguity. The grand potential Ω_V (2.1) is divided into a bulk and surface contribution

$$\Omega_V = \Omega_b + \Omega_{ex} = -pV_v + \Omega_{ex} \tag{2.29}$$

where V_v is the volume occupied by the bulk vapor phase and Ω_{ex} is the surface contribution to Ω_V. Combining (2.1), (2.8), and (2.29)

$$\frac{\Omega_{ex}}{4\pi R^2} = \frac{1}{R^2}\int_R^\infty u^2\left[p - p_h(\rho(u)) + \left(\frac{1}{2}\right)\rho(u)(\mu_h(\rho(u)) - \mu) + \left(\frac{1}{2}\right)\rho(u)\, V_{ext}(u)\right] du \tag{2.30a}$$

which, after some algebra, is reduced to

$$\frac{\Omega_{ex}}{4\pi R^2} = \frac{1}{2\alpha}\left\{\epsilon_W(\mu - \mu_h(R) - V_{ext}(R)) - \mu'_h(R)(\mu - \mu(R)) + \frac{2}{3R^2}\int_R^\infty u^2 \mu'^2_h(u)\left[1 + 2\frac{R^3}{u^3}\right]\right\} \tag{2.30b}$$

3. Numerical Calculations and Discussion

The boundary value problem in (2.11) and (2.12) was solved numerically for $T = 0.8$ and a wide range of values of R and ϵ_W; the solution is the equilibrium density profile as a function of the radial distance from the origin of spherical wall.

To solve (2.11) and (2.12) numerically, the upper bound (the limit $r \to \infty$) is replaced by an, as yet, unknown finite bound R_T, which will be treated as an additional dependent variable, thus increasing the number of first-order differential equations from two to three, since R_T will be calculated together with the solution of the boundary value problem. Consequently, the boundary conditions in (2.12b) now reads

$$\eta(R_T) = \eta_V, \quad \eta'(R_T) = 0 \tag{3.1}$$

To facilitate the solution of the system of diffential equations the variables (r,η,η') are replaced by $(t,z,\dot{z})$; the dot denotes a derivative with respect to the new independent variable t, which takes values within the interval [0,1]. The change from r to t can be effected by means of

$$r - R = tz_3, \quad \dot{z}_3(t) = 0 \tag{3.2}$$

where $z_3 := R_T - R$. The system of first-order differential equations replacing (2.11) is[11]

$$\dot{z}_1(t) = z_3 z_2(t)$$

$$\dot{z}_2(t) = \left[-\frac{2}{R + tz_3} z_2(t) - B_1(z_1)z_2^2(t) - B_2(z_1) - B_3(z_1)z_1(t)\right] z_3 \tag{3.3}$$

$$\dot{z}_3(t) = 0$$

$$\dot{z}_4(t) = 0$$

where $z_4(t) := \eta(0)$, the wall density, treated as an additional dependent variable to facilitate the solution of the boundary value problem (3.3), $z_1(t) := \eta(R + tz_3)$, and $z_2(t) := \eta'(R + tz_3)$; the boundary conditions (2.12) take the form

$$z_2(0) = \left\{(\mu_h[z_1(0)] - \mu)\left(\coth R - \frac{1}{R}\right) - \epsilon_W\right\} \Big/ A_1(z_1(0)) \tag{3.4}$$

$$z_1(0) = z_4(0), \quad z_1(1) = \eta_v, \quad z_2(1) = 0$$

The direct dependence of the wall strength on R influences considerably the values assumed by ϵ_W for a specific R; for small values of R, ϵ_W cannot take very small values since, then, the attraction strength will be very weak, for it is radius-dependent, whereas the contrary is true for larger values of R. The density profiles, for any values of R and ϵ_W, exhibit a monotonic decrease or increase from the wall value $\eta(0)$ toward the bulk density η_V, implying either wetting (growth of thin or thick films, depending on the value of ϵ_W) or nonwetting of the wall. The growth of an infinitely thick film on it (complete wetting) would require an infinite contribution to the free energy of the system,[6] see also the Antonov rule (1.3, 1.4), since the radius R of the substrate is finite (Figure 1a,b). A comparison can be drawn between the above behavior and that shown in the presence of a planar substrate. For a planar substrate, if the thickness of the wetting layer diverges as coexistence is approached, the system is in wetting class I, if it remains finite it is in class II, and if it is nonwet it is in class III; the wetting diagram is identical to the phase diagram because ϵ_W and α are related to the equilibrium densities[1,2] (Figure 2). Also, in this geometry a film can be of finite thickness when the system is in wetting class II (even at coexistence) or in class I but the bulk vapor phase is undersaturated. A film grown on a spherical substrate can be considered, with regard to its thickness,

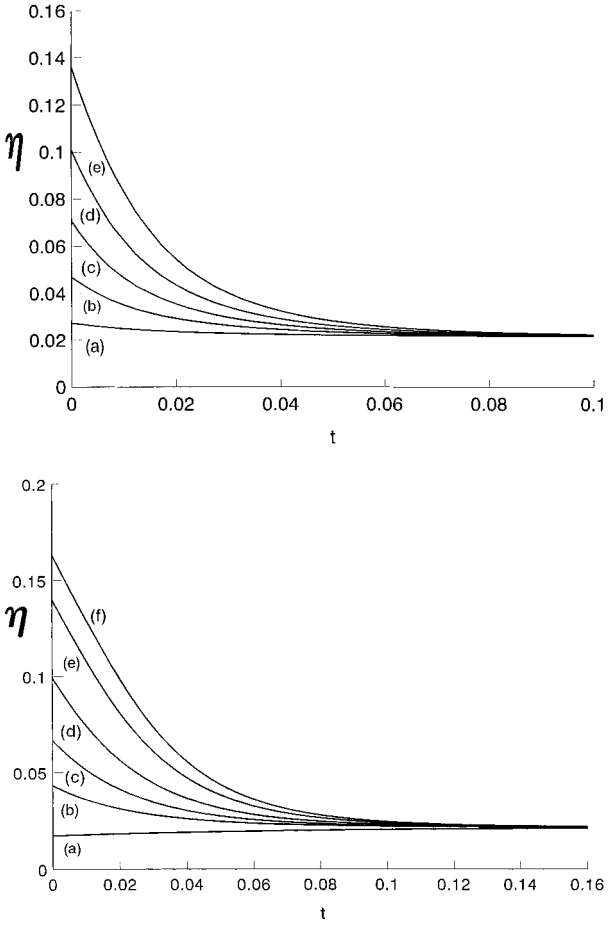

Figure 1. Packing fraction profile $\eta(t)$ as a function of reduced distance t. (a) Curves a, b, c, d, and e are for $R = 2$ and $\epsilon_W = 0.8$, 2, 3, 4, and 5, respectively. t varies within the interval [0,1]. The thin−thick transition becomes manifest as ϵ_W increases. Curves a, b, c, d, e, and f are for $R = 30$ and by $\epsilon_W = 0.1$, 2, 3, 4, 5, and 5.5, respectively Curve a corresponds to nonwetting by the liquidlike phase (drying, class III).

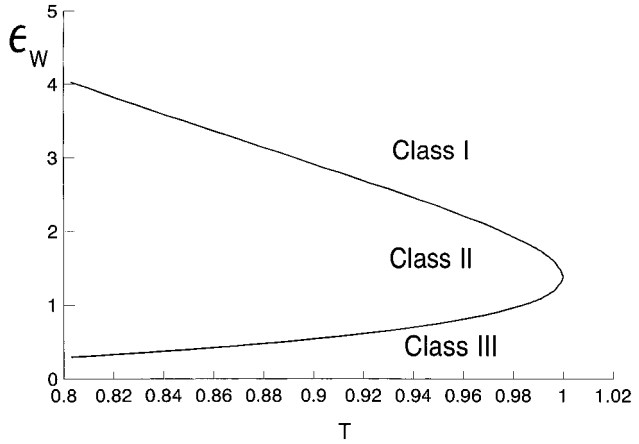

Figure 2. Wetting diagram of the current model fluid. The boundaries between the three wetting classes are determined by the equilibrium values of the vapor and liquid densities.

equivalent to a film in the presence of a planar substrate when the system is either in class II or in class I but undersaturated.[2]

For a small wall's radii, the density profiles, for a specific R, exhibit only thin-film growth for small ϵ_W's, which turns into thick-film growth as ϵ_W increases (Figure 1a); in this case, adsorption Γ is always positive and increasing (Figure 3). For larger radii, ϵ_W can assume smaller values for which $\eta(0)$ is smaller than η_V and the respective density profile is an

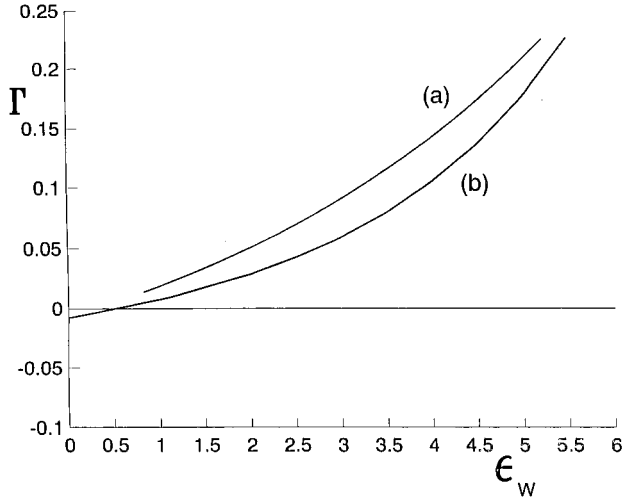

Figure 3. Adsorption Γ for the wall−vapor interface as a function of ϵ_W for $R = 2$ (a) and 30 (b). The negative values of Γ correspond to nonwetting for very small ϵ_W.

increasing, nonwetting case (Figure 1b); as ϵ_W increases $\eta(0)$ becomes greater than η_V, and a thin-film grows on the substrate (transition from nonwetting to wetting), which becomes thick on increasing ϵ_W further. In this case, adsorption Γ, being initially negative, becomes positive and finite as ϵ_W increases but never diverges because class I is excluded (Figure 3). The wall-value $\eta(0)$ of the density, at fixed R, varies considerably as ϵ_W increases, an outcome of Figure 1a,b and other numerical calculations not presented here, since increasing ϵ_W, at fixed T, promotes wetting because of the increase of the wall−vapor attractive interaction.[1,2]

These results are in accord with earlier theories regarding the thickness of the wetting layers formed on a sphere.[4−6] However, Holyst and Poniewierski[4] studied only the large-R behavior employing the double-parabola approximation, which breaks down when the temperature is close to the bulk critical point T_c; they concluded that only thin and thick films can grow on a sphere. A similar result was also found by Gelfand and Lipowski,[5] who employed the same approximation to a Landau-type theory, exploiting the small curvature regime, $R \ll \xi$, where ξ is the bulk correlation length; this theory was generalized by Upton et al.,[6] who calculated only the global phase diagram for adsorption phase transitions.

The continuous increase of Γ with ϵ_W, at fixed T and R, derives from corresponding increase in the wall−vapor attractive interaction. Increasing Γ means a continuous deposit of bulk-gas particles in the wall−vapor interfacial region, whereby a thin or thick film is formed; the wall is wet by a liquidlike phase ($\eta(0) > \eta_V$), while for very small ϵ_W this phase is excluded by the substrate ($\eta(0) < \eta_V$, drying transition) making the coverage Γ negative.

The behavior of the pressure-tensor components is completely different from that of a spherical drop[7] where, for small supersaturations, both components are equal at the center of the drop and over a distance inside it, implying the existence of a bulk liquid phase inside the drop. In the transition region, initially, $p_T(r)$ becomes significantly smaller than $p_N(r)$, and the interface is under tension, displaying a deep lobe, which for the smaller supersaturations acquire a small negative part. After the minimum value, $p_T(r)$ becomes noticeably larger than $p_N(r)$, the interface now is under compression, and both tensors join smoothly in the bulk region). For the spherical substrate, both components, the transverse $p_T(r)$ and the normal $p_N(r)$, do not satisfy any symmetry relation apart from the requirement to tend to p_V as $r \rightarrow \infty$. Their values on the substrate are

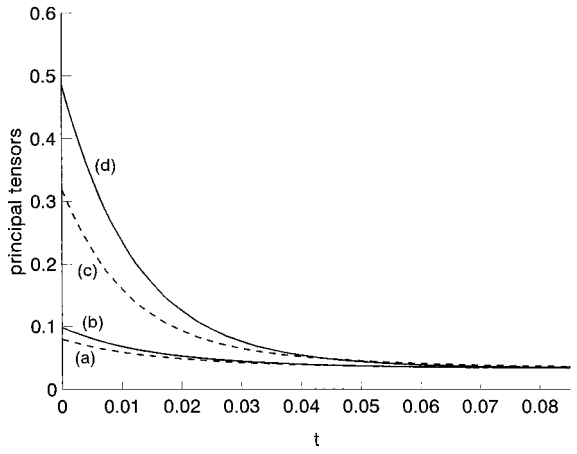

Figure 4. Transverse tensor $p_T(r)$, dashed line, and the normal tensor $p_N(r)$, full line, as functions of the reduced distance t, for $R = 30$. $\epsilon_W = 1$ for curves a, b, and $\epsilon_W = 5$ for curves c, d. The interface is mainly under tension, $p_N > p_T$; the region where it is under compression, $p_N < p_T$, is just visible.

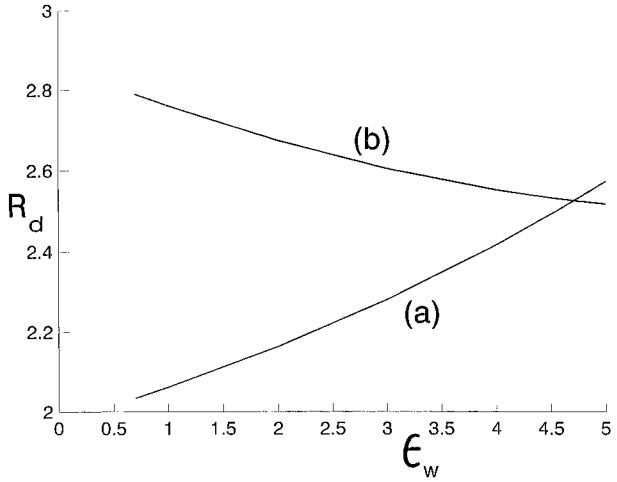

Figure 5. Equimolar radius R_e (a) and the radius of tension R_s (b) as functions of ϵ_W for $R = 2$.

different as well as in the transition region. The $p_N(r)$ component is greater than the transverse $p_T(r)$ ($p_N(r) > p_T(r)$) whereas the region where $p_N(r) < p_T(r)$ is not as easily noticeable as in a spherical drop or planar wall;[7] thus the interface is, mainly, under tension (Figure 4).

Other important quantities, closely related with the pressure tensor, are the surface tension (which is now different from the total surface excess grand potential when an external field is present) and the pressure difference Δp (2.18).

To make possible the calculation of the surface tensions, initially the radius R_S of the surface of tension and the equimolar radius R_e are calculated from (2.25) and (2.26), respectively; their plots appear in Figure 5 for $R = 2$.

For any substrate, R_S and R_e differ significantly for small values of ϵ_W (Figure 5). R_S always decreases as ϵ_W increases, because for small ϵ_W's the adsorbed phase is very diffused around the substrate (the wall−fluid attraction is very small) and $\eta_V < \eta(0) \ll \eta_L$, while for higher ϵ_W's the adsorbed phase becomes denser, $\eta(0)$ tends toward η_L and is more localized around the wall, because of stronger attraction, thus driving R_S to smaller values, and it seems it attains an asymptotic value for very large ϵ_W's. On the other hand, R_e increases with ϵ_W because it is related, by its definition, to the amount of adsorbed particles that increase in number with ϵ_W, resulting in increasing R_e.

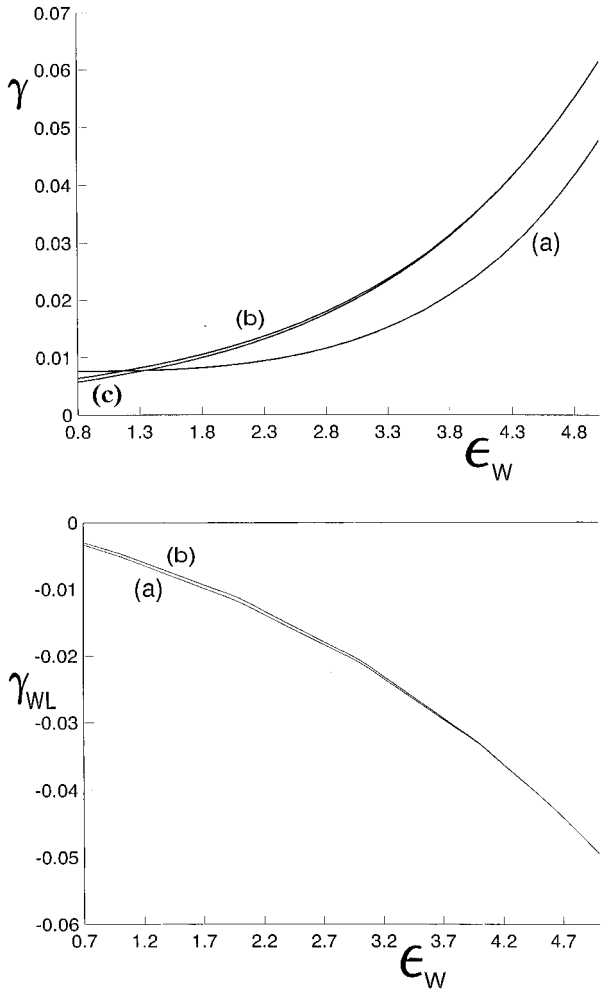

Figure 6. (a) Surface tensions as functions of ϵ_W for $R = 2$: (a) wall−vapor, (b) equimolar, (c) mechanical. (b) Wall−liquid surface tensions as functions of ϵ_W for $R = 2$: (a) equimolar, (b) mechanical.

Although the radii R_S and R_e behave differently, the associated surface tensions γ_S and γ_e do not. For any substrate both increase with ϵ_W; for small ϵ_W's they vary slowly as well as the wall−vapor tension γ_{WV}. For small wall radii (e.g., $R = 2$, Figure 6a), they are different for small and moderate ϵ_W's, while they coincide for high ϵ_W's; however, for higher R's both tensions are practically coincident for any ϵ_W. The wall−vapor tension γ_{WV} (Figure 6a) for small ϵ_W's is higher than γ_S and γ_e because the wall−fluid attraction is small and more work is needed to create the respective interface while for higher ϵ_W's γ_{WV} becomes smaller than γ_S or γ_e. The other component of γ_{WV}, i.e., γ_{WL}, is negative and decreases as ϵ_W increases (Figure 6b). For larger wall radii, the respective surface tensions practically coincide for any ϵ_W.

In the earlier theories[4−6] there are not calculations concerning the adsorption, pressure tensor components, surface tensions, and their associated radii; thus, no attempt is made to make any comparison with these theories. Only in Holyst and Poniewierski[4] are there some expressions for the wall−vapor surface tension, but there are not any comments about its behavior.

4. Conclusion

The mean-field density functional approach, originally introduced by Sullivan[1] for the study of wetting of a planar wall by a bulk fluid, is generalized for the case of a spherical wall embedded in a bulk vapor phase. The results of current theory

are in accordance with conclusions drawn by earlier theories employing different models. Namely, wetting takes place in the form of thin or thick films, or nonwetting, depending on the value of the parameter ϵ_W. Gradual change in ϵ_W can cause wetting to move from one form to another. The behavior predicted by the various theories can provide convincing explanations, at least qualitative, about the factors controlling film growth, i.e., temperature, substrate strength and radius, and intermolecular forces, which in some cases have been observed in experimental situations. Also, by adjusting the parameters of the model suitably, it may be proved usable to give a qualitative and, to some extent, quantitative description of experimental results (adsorption, surface tensions, dividing radii, pressure tensor) for the condensation of simple fluids in the presence of spherical substrates, as for planar walls or the van der Waals model for bulk fluids.

The present model can also be considered as an essential framework on which more refined treatments (different inverse-range parameters, $\lambda \neq \lambda_w$, smoothed- and weighted-density approximation) will be based, although these refinements do not influence significantly the integrated quantities (adsorption, surface tensions, dividing radii, etc.) but give a better picture of the density oscillations close to the wall (smoothed- and weighted-density approximation[12]) or change the order of the wetting transition[13] ($\lambda \neq \lambda_w$), as is well-known for a planar wall.

The current model belongs to the class of short-range forces (SRF), for which the wetting transition is always second order, when the inverse range parameters of the fluid−fluid (λ_{FF}) and wall−fluid (λ_{WF}) are equal[1] and critical wetting is expected (except for special choices of the wall−fluid energies[14]). If the long-range forces (LRF) are present, the wetting transition is first order as well as in the current model when $\lambda_{FF} \neq \lambda_{WF}$.[13] However, the presence of LRF may also inhibit a wetting transition.[15]

A similar case of only partial wetting appears in Durian and Franck,[9] in their study of adsorption of a critical binary mixture (carbon disulfide + nitromethane) at coexistence on borosilicate glass substrates prepared differently. Heavily silylated surfaces adsorb the carbon disulfide-rich phase (nonpolar molecule) at short ranges, and there is no a transition from partial to complete wetting for any $T < T_c$, because of the competetion of LRF favorable to the nitromethane-rich phase and SRF favorable to the carbon disulfide-rich phase.

References and Notes

(1) Sullivan, D. E. *Phys. Rev. B* **1979**, *20*, 3991; *J. Chem. Phys.* **1981**, *74*, 2604.

(2) Hadjiagapiou, I.; Evans, R. *Mol. Phys.* **1985**, *54*, 383.

(3) Sullivan, D. E.; Telo da Gamma, M. M. Wetting Transitions and Multilayer Adsorption at Fluid Interfaces. In *Fluid Interfacial Phenomena*; Croxton, C. A., Ed.; Wiley: New York, 1986; Chapter 2.

(4) Holyst, R.; Poniewierski, A. *Phys. Rev. B* **1987**, *36*, 5628.

(5) Gelfand, M. P.; Lipowski, R. *Phys. Rev. B* **1987**, *36*, 8725.

(6) Upton, P. J.; Indekeu, J. O.; Yeomans, J. M. *Phys. Rev. B* **1989**, *40*, 666.

(7) Hadjiagapiou, I. *J. Phys.: Condens. Matter* **1994**, *6*, 5305; **1995**, *7*, 547.

(8) Steele, W. A. *The Interaction of Gases with Solid Surfaces*; Pergamon Press: Oxford, 1974; Chapter 2.

(9) Durian, D. J.; Franck, C. *Phys. Rev. Lett.* **1987**, *59*, 555.

(10) Rowlinson, J. S.; Widom, B. *Molecular Theory of Capillarity*; Clarendon Press: Oxford, 1982; Chapter 4.

(11) Stoer, J.; Bulirsch, R. *Introduction to Numerical Analysis*; Springer-Verlag: New York, 1983; Chapter 7.

(12) Tan, Z.; Marini Bettolo Marconi, U.; van Swol F.; Gubbins, K. *J. Chem. Phys.* **1989**, *90*, 3704.

(13) Teletzke, G. F.; Scriven, L. E.; Davis, H. T. *J. Chem. Phys.* **1982**, *77*, 5794; **1983**, *78*, 1431. Tarazona, P.; Evans, R. *Mol. Phys.* **1983**, *48*, 799.

(14) Indekeu, J. O. *Phys. Rev. B* **1987**, *36*, 7296.

(15) de Gennes, P.-G. *J. Phys. (Paris) Lett.* **1981**, *42*, L377.